Received: 18 December 2018 | Revised: 21 March 2019 | Accepted: 20 May 2019

DOI: 10.1111/bph.14754

RESEARCH PAPER

Inhibition of polycomb repressor complex 2 ameliorates neointimal hyperplasia by suppressing trimethylation of H3K27 in vascular smooth muscle cells

Jing Liang[1] | Qi Li[1] | Wenbin Cai[1] | Xuejiao Zhang[1] | Bing Yang[2] | Xin Li[3] | Shuai Jiang[1] | Shanshan Tian[4] | Kai Zhang[4] | Hao Song[1] | Ding Ai[1] | Xu Zhang[1] | Chunjiong Wang[1] | Yi Zhu[1]

[1] Collaborative Innovation Center of Tianjin for Medical Epigenetics, Tianjin Key Laboratory of Medical Epigenetics, and Department of Physiology and Pathophysiology, Tianjin Medical University, Tianjin, China

[2] Department of Cell Biology, Tianjin Medical University, Tianjin, China

[3] Department of Pharmacology, Tianjin Medical University, Tianjin, China

[4] Department of Biochemistry and Molecular Biology, Tianjin Medical University, Tianjin, China

Correspondence
Yi Zhu, Chunjiong Wang, and Xu Zhang, Department of Physiology and Pathophysiology, Tianjin Medical University, Tianjin 30070, China.
Email: zhuyi@tmu.edu.cn; wangchunjiong@tmu.edu.cn; xuzhang@tmu.edu.cn

Funding information
National Natural Science Foundation of China, Grant/Award Numbers: 91539108, 81790621, 81770836, 81822006 and 81730014

Background and Purpose: The increased proliferation and migration of vascular smooth muscle cells (VSMCs) after arterial injury contributes greatly to the pathogenesis of neointimal hyperplasia. As a major component of epigenetics, histone methylation plays an important role in several cardiovascular diseases. However, its role in restenosis is still unclear.

Experimental Approach: Human aortic VSMCs were challenged with PDGF-BB, and total histones were extracted and analysed by HPLC/MS. For the in vivo study, rats were subjected to wire-guided common carotid injury.

Key Results: PDGF-BB markedly increased the H3K27me3 level, as demonstrated by use of HPLC/MS and confirmed by western blot analysis. Enhancer of zeste homologue 2 (EZH2), the histone H3K27 methyltransferase component of polycomb repressive complex 2, was also up-regulated by PDGF-BB in VSMCs, and in the neointimal hyperplasia induced by wire injury of the rat carotid artery. Furthermore, inhibiting H3K27me3 by treatment with 3-μM UNC1999, an EZH2/1 inhibitor, significantly suppressed PDGF-BB-induced VSMC proliferation compared with the PDGF-BB-treated group. Consistently, neointimal formation was significantly attenuated by oral or perivascular administration of UNC1999 compared with the sham group. Mechanistically, the increase in H3K27me3 inhibited the transcription of the cyclin-dependent kinase inhibitor $p16^{INK4A}$ and thus promoted VSMC proliferation.

Conclusions and Implications: Vascular injury elevated the expression of EZH2 and the downstream target H3K27me3, which suppressed $p16^{INK4A}$ expression in VSMCs and promoted VSMC proliferation and neointimal hyperplasia. EZH2 inhibition might be a potential therapeutic target for restenosis.

Abbreviations: EZH2, enhancer of zeste homologue 2; H3K27, histone H3 lysine 27; H3K27me3, trimethylation of H3K27; $p16^{INK4A}$, cyclin dependent kinase inhibitor 2A; PRC2, polycomb repressive complex 2; SM-22α, smooth muscle protein 22-α; VSMC, vascular smooth muscle cell; α-SMA, α-smooth muscle actin

Jing Liang and Qi Li equally contributed to this work.

1 | INTRODUCTION

Atherosclerosis, a chronic inflammation of the arteries, is the trigger of various cardiovascular diseases. The primary complications of atherosclerosis, including coronary heart disease, stroke, and peripheral arterial disease, ascertain that it is the most common cause of death due to vascular disorders (Herrington, Lacey, Sherliker, Armitage, & Lewington, 2016). Angioplasty is a highly effective treatment for narrowing of the coronary arteries. However, restenosis after angioplasty, the healing response of the arterial wall to mechanical injury, greatly dampens the satisfactory prognosis of atherosclerosis (He et al., 2018; Liu, Bauer, & Martin, 2016). The main pathogenesis of restenosis is neointimal hyperplasia and vessel remodelling. Robust proliferation and migration of vascular smooth muscle cells (VSMCs) after arterial injury greatly contributes to neointimal hyperplasia (Liu et al., 2016). Therefore, investigating the mechanism of altered VSMC behaviour is vital to understanding the process of neointimal hyperplasia and developing new strategies for the prevention and treatment of restenosis.

Epigenetics, which involves the manipulation of gene expression via chemical modification of DNA or chromatin proteins without sequence alteration, is widely involved in the pathogenesis of multiple cardiovascular diseases (Cao et al., 2014). Histone methylation is one of the major mechanisms that alter chromatin architecture, accompanied by altered gene expression (Dambacher, Hahn, & Schotta, 2010). The major histone methylation sites are numerous lysines located within the N-termini of histones as well as the nucleosome core region, mainly H3K4, H3K9, H3K27, H3K36, and H4K20 (Dambacher et al., 2010). Histone methylation plays an important role in dilated cardiomyopathy, heart failure, cardiac hypertrophy, and atherosclerosis (Cao et al., 2014; Leentjens et al., 2018).

Polycomb repressive complex 2 (PRC2) is essential for H3K27 di/trimethylation (Conway, Healy, & Bracken, 2015). This complex is closely associated with cell differentiation, development, and various cancers (Moritz & Trievel, 2018). The methyltransferase core, enhancer of zeste homologue 2/1 (**EZH2/1**), is the core component of PRC2, found to be involved in heart development, pulmonary arterial hypertension, and aortic dissection (Ai et al., 2017; Aljubran et al., 2012; Li et al., 2018). However, whether PRC2-mediated methylation of H3K27 is involved in restenosis post-angioplasty is unknown.

UNC1999 (*N*-[(1,2-dihydro-6-methyl-2-oxo-4-propyl-3-pyridinyl) methyl]-1-(1-methylethyl)-6-[6-[4-(1-methylethyl)-1-piperazinyl]-3-1*H*-indazole-4-carboxamide) is a specific inhibitor of EZH2/1. It binds to the *S*-adenosyl-L-methionine (**SAM**)-binding site within EZH2/1 through hydrogen bonds and hydrophobic interactions and thus disrupts the association between EZH2/1 and SAM followed by H3K27me3 reduction (Konze et al., 2013). Moreover, it is orally bioavailable. It has been demonstrated that a single 50 mg·kg^{-1} oral dose of UNC1999 achieves a high C_{max} (4,700 nM). The plasma concentration of UNC1999 declines at 8 hr and is maintained above its cellular IC_{50} for 20 hr (Konze et al., 2013). Thus, it is a useful tool to investigate the role of EZH2/1 in vivo.

What is already known

- EZH2/1-mediated upregulation of H3K27me3 is involved in heart development, pulmonary arterial hypertension, and aortic dissection.

What this study adds

- H3K27 trimethylation in VSMCs is positively associated with restenosis.
- EZH2-mediated up-regulation of H3K27me3 promotes the proliferation of VSMCs and restenosis by repressing $p16^{INK4A}$.
- The EZH2/1 inhibitor UNC1999 can attenuate restenosis by reducing the H3K27me3 level followed by $p16^{INK4A}$ recovery.

What is the clinical significance

- EZH2 might be a potential therapeutic target for restenosis.

To explore the role of histone methylation in neointimal hyperplasia, we used quantitative MS of histones and demonstrated their methylation in VSMCs treated with **PDGF-BB**. PDGF-BB increased H3K27 trimethylation (H3K27me3) level in VSMCs. Moreover, the levels of H3K27me3 and EZH2 were increased in rat injured carotid arteries and PDGF-BB-treated human VSMCs. In VSMCs, PRC2 inhibition by UNC1999 significantly suppressed the migration and proliferation of VSMCs induced by PDGF-BB. Accordingly, systemic and perivascular application of UNC1999 greatly ameliorated wire injury-induced restenosis. Mechanistically, this therapeutic effect of UNC1999 was associated with de-repressed expression of the cyclin-dependent kinase inhibitor $p16^{INK4A}$. Our study demonstrated a novel role of epigenetic regulation in vascular injury-induced VSMC proliferation and neointimal hyperplasia, which suggests that restenosis can be ameliorated by inhibiting EZH2.

2 | METHODS

2.1 | Cell culture

Human aortic VSMCs were purchased from FDCC (Shanghai, China) and cultured in DMEM-F12 (Thermo Fisher Scientific Corp., Waltham, MA, USA) complete medium (DMEM-F12, 10% FBS, recombinant human EGF, insulin-like growth factor, and ascorbic acid). Cells were passaged at 90% confluence and maintained in a humidified incubator at 37°C with 5% CO_2. Cells from passages 5 to 7 were used for experiments. Before treatment, VSMCs were starved by incuabating them in serum-free medium for 48 hr for de-dedifferentiation.

2.2 | Experimental animals and carotid wire-guided injury model

Specific-pathogen-free male Sprague–Dawley rats (~200 g) were obtained from the Experimental Animal Centre of Military Medical Science Academy (RRID:RGD_734476; Beijing, China). All rats were housed in a temperature-controlled environment in cages containing with wood shavings as bedding (two to three per cage) with 12-hr light/dark cycles and received food and water ad libitum. Carotid wire-guided injury was used to model restenosis (Wang et al., 2015). Briefly, 0.1% heparin sodium was injected via the tail vein of rats at 0.1 mg.100·g^{-1} body weight to avoid thrombosis. Rats were anaesthetized with isoflurane (the induction dose was 3% in oxygen for 3 min, and the maintenance dose was 2.5% in oxygen during the operation). After the carotid artery had been isolated, a 0.83-mm wire was introduced through the left external artery and advanced back and forth, about 3 cm proximally, five times with gentle rotation. The left external artery of the sham group was isolated and opened as for the surgery group but without wire injury. After surgery, the opening was sewed up followed by disinfection with iodine (2%). The rats were placed on a heated operating table to maintain body temperature until they recovered from the anaesthetic. Rats were randomized into different groups in the study. The investigator was not blind to the experimental groups. All procedures involving experimental animals were performed under the principle for replacement, refinement, or reduction (the 3Rs) and in accordance with U.S. National Institutes of Health Guide for the Care and Use of Laboratory Animals (NIH Publication No. 85-23, updated 2011) and were approved by the Institutional Animal Care and Use Committee of Tianjin Medical University (Tianjin, China). Animal studies are reported in compliance with the ARRIVE guidelines (Kilkenny et al., 2010) and with the recommendations made by the *British Journal of Pharmacology*.

2.3 | UNC1999 application

For gastric gavage, UNC1999 (Selleck Chemicals, Houston, TX, USA) was dissolved as described previously (Konze et al., 2013). UNC1999 was dissolved in 0.5% sodium carboxymethylcellulose and 0.1% Tween-80 in sterile water. The dosage of UNC1999 was 50 mg·kg^{-1} body weight·day^{-1}. UNC1999 was applied to the UNC1999 group, and an equivalent amount of vehicle was applied to the sham and surgery-only groups from 1 day pre-surgery to 2 weeks post-surgery. Then, rats were killed, and the left common carotid arteries were collected for analysis.

For perivascular application, UNC1999 was dissolved in DMSO at 50 mg·ml^{-1}. The dose for the perivascular application of UNC1999 was 50 mg·kg^{-1} body weight mixed with 30% PF127 gel (Sigma Aldrich, St. Louis, MO, USA) as described previously (Jain, Singh, Singh, & Barthwal, 2015; Wang et al., 2009). After isolation of the left common carotid artery, the mixture of UNC1999 and PF127 gel was applied perivascularly to the UNC1999 group, and the mixture of DMSO and PF127 was applied to the sham and surgery-only groups. After recovery, rats were transferred to normal feeding conditions and kept for 2 weeks. Then, rats were killed, and the left common carotid arteries were collected for analysis.

2.4 | BP measurements

BP was monitored by a tail-cuff system (Softron BP-98A; Softron, Tokyo, Japan), and the values were averaged from at least five consecutive measurements per rat. UNC1999 (50 mg·kg^{-1} body weight·day^{-1}) was administered to the rats by gavage for 3 days, and BP was tested for four sequential days starting from Day 1 before the administration of UNC1999.

2.5 | Determination of histone modification by MS

H3 histones were extracted and analysed as described previously (Yuan et al., 2015; Zhang et al., 2015). Briefly, total H3 histone proteins were extracted by the acid extraction method and resolvedby use of a 15% SDS-PAGE gel. After coomassie blue staining, the bands of interest were excised and subjected to in-gel digestion. The peptide extracts obtained were processed and analysed by quantitative MS (NANO-HPLC/MS; Eksigent Technologies, Dublin, CA/Thermo Fisher Scientific Corp.).

2.6 | MTS assay

VSMCs were seeded in 96-well plates (5 × 10^3 per well) in complete DMEM-F12 medium, then starved for 48 hr by incubation in serum-free DMEM. Then, cells were treated with PDGF-BB (40 ng·ml^{-1}) with or without 3-μM UNC1999 for 36 hr. A treatment of 10–50 ng·ml^{-1} PDGF-BB for 24–48 hr was reported to induce VSMC proliferation (Cai et al., 2015; Igata et al., 2005; Li et al., 2018; Liu et al., 2014; Song et al., 2018; Wang et al., 2018). Thus, for the MTS assay and other in vitro experiments, we treated the VSMCs with 40 ng·ml^{-1} of PDGF-BB for 36 hr. UNC1999 was dissolved in DMSO, and the control groups were treated with the same volume of DMSO. MTS reagent (Biovision, Milpitas, CA, USA) was added (20 μl per well) and the samples were incubated at 37°C for 4 hr. The plate was shaken on a shaker briefly, then underwent absorbance measurement by using a plate reader set at 490 nm.

2.7 | Cell cycle determination by flow cytometry

Treated VSMCs were trypsinized and centrifuged at 150× *g* for 5 min and washed in PBS three times. Cells were re-suspended in 0.5 ml of pre-cooled PBS and fixed with 4.5 ml of 70% ethanol at 4°C for 2 hr. Cells were then washed with ice-cold PBS twice. The cell pellets obtained were resuspended with 10 μg·ml^{-1} propidium iodide (Beyotime Biotechnology, Shanghai, China) then incubated at 37°C in the dark for 10 min. Then, the cell suspension was analysed by flow cytometry (BD FACSVerse; BD Biosciences, San Jose, CA, USA).

2.8 | Cell migration assays

Cell migration was analysed by transwell and scratching healing assays. For the transwell assay, treated VSMCs were seeded in the upper chamber at 1×10^4 cells, and DMEM with 2.5% FBS was placed in the lower chamber. After 4-hr incubation, cells in the transwells were fixed with 4% paraformaldehyde for 15 min. Cells attached in the upper chamber were removed gently, and cells attached in the lower chamber were stained with DAPI. Images were captured under an inverted microscope. For the scratch-healing assay, after de-dedifferentiation of cells and the corresponding treatments, straight gaps were introduced to cells in the centre of the plate wells in complete medium. After 12 hr, the gap width was measured under an inverted microscope (Leica DFC-450, Wetzlar, Germany).

2.9 | Immunofluorescence staining

Tissue or cell slides were rinsed with PBS for 5 min, fixed with 4% paraformaldehyde for 15 min, penetrated with 0.1% Triton X-100 solution for 15 min, and blocked with 1% BSA for 1 hr at room temperature. Primary antibodies for H3K27me3 (1:300, cat#: 07449, RRID:AB_310624; Millipore, Burlington, MA, USA), Ki67 (1:200, cat#: 11882, RRID:AB_2687824; CST, Danvers, IL, USA;), $p16^{INK4A}$ (1:50, cat#: 108831, RRID:AB_2078303; Proteintech, Rosemont, IL, USA), and α-smooth muscle actin (α-SMA; 1:400, cat#: A2547, RRID:AB_476701; Sigma Aldrich) were incubated with tissue sections or cell slides at 4°C overnight, then secondary antibodies (goat anti-mouse IgG, 1:200, cat#: A11032, RRID:AB_2534091; goat anti-rabbit IgG, 1:200, cat#: A11034, RRID:AB_2576217; Invitrogen, Carlsbad, CA, USA) were applied at room temperature for 1 hr followed by slide mounting with DAPI-containing mounting medium. Images were captured under a Zeiss confocal microscope (Axio-Imager LSM-800, Oberkochen, Germany). The Immuno-related procedures used comply with the recommendations made by the *British Journal of Pharmacology*.

2.10 | Elastic tissue fibres-Verhoeff's van Gieson staining (EVG)

Elastic tissue was demonstrated by use of an EVG staining kit according to the manufacturer's instructions (Sigma Aldrich). Images were captured under an inverted microscope (Leica DFC-450, Wetzlar, Germany).

2.11 | Western blot analysis

Proteins from VSMCs or rat carotid arteries were resolved by 10% or 12% SDS-PAGE and transferred to PVDF membranes, which were blocked with 5% non-fat milk for 2 hr at room temperature, then incubated with primary antibodies for H3K27me3 (1:5,000, cat#: 07449), EZH1 (1:2,500, cat#: ABE281), and EZH2 (1:1,000, cat#: 07689, RRID:AB_417397; all from Millipore); total H3 (1:3,000, cat#: 4499, RRID:AB_10544537) and PCNA (1:1,000, cat#: 2586, RRID:AB_2160343; both from CST); α-SMA (1:8,000, cat#: A2547; Sigma Aldrich); smooth muscle protein 22-α (SM-22α; 1:500, cat#: SC-53932, RRID:AB_1129519) and α-tubulin (1:1,000, cat#: SC-8035, RRID:AB_628408; both from Santa Cruz Biotechnology, CA, USA); and GAPDH (1:10,000, cat#: 600041, RRID:AB_2107436; Proteintech) at 4°C overnight, then secondary antibodies (goat anti-mouse IgG, 1:5,000, cat#: 4741806, RRID:AB_2307348; goat anti-rabbit IgG, 1:5,000, cat#: 0741506, RRID:AB_2721169; KPL, Gaithersburg, MD, USA) were applied at room temperature for 1 hr. Protein blots were visualized by using an enhanced chemiluminescence western blotting detection kit (Thermo Fisher Scientific Corp.) and analysed by using ImageJ software (RRID:SCR_003070).

2.12 | Quantitative real-time PCR (qPCR)

Total RNA was extracted by using a kit (Transgene, Beijing, China). RNA was reverse-transcribed into cDNA by using a reverse transcription kit (Thermo Fisher Scientific Corp.). qPCR was performed with SYBR Green PCR master mix (Transgene, Beijing, China) and followed the Minimum Information for Publication of Quantitative Real-Time PCR Experiments guidelines. The expression of genes was normalized to that of GAPDH. All primers were designed by using Primer 3.0 (Table S1).

2.13 | Chromatin immunoprecipitation (ChIP)

The ChIP assay was performed as described previously (Li et al., 2017; Yao et al., 2016). Briefly, VSMCs were treated with 40 $ng \cdot ml^{-1}$ PDGF-BB for 36 hr. Cells were cross-linked with 1% formaldehyde before being re-suspended with SDS lysis buffer. Chromatin fragments of 200–500 bp were generated by high-power sonication for seven cycles of 30-s ON and 30-s OFF. The length of the sonication product was examined by agarose gel electrophoresis. Anti-H3K27me3 antibody was added to the sonication product and gently rotated at 4°C for 12 hr. Then, magnetic beads (Thermo Fisher Scientific Corp.) were added to the immunoprecipitation (IP) complex and incubated with gentle rotation at 4°C for 4 hr. Thereafter, the bead–IP complex was rinsed with ChIP buffer sequentially, followed by cross-linking reversal. Precipitated genomic DNA was amplified by qPCR and normalized to input DNA. Primers were as previously reported (Maruo et al., 2011) and are in Table S1. Data were from three independent experiments ($n < 5$) and were not subjected to statistical analysis.

2.14 | Data and statistical analysis

Data are presented as mean ± SEM, and two or more groups were compared by Student's *t* test or one-way ANOVA (GraphPad Prism 5, RRID:SCR_002798; GraphPad Software, Inc.). For one-way ANOVA, Bonferroni's multiple comparison post hoc test was performed only when F achieved $P < .05$, and there was no significant variance inhomogeneity. Statistical significance was set at $P < .05$. The data and statistical analysis comply with the recommendations of the

British Journal of Pharmacology on experimental design and analysis in pharmacology (Curtis et al., 2018).

2.15 | Materials

UNC1999 was from Selleck Chemicals. PF127 gel was from Sigma Aldrich. MTS reagent was from Biovision. Propidium iodide was from Beyotime Biotechnology, Shanghai, China. EVG staining kit was from Sigma Aldrich. **Cycloheximide** was from Cell Signaling Technology. Antibodies for H3K27me3 and EZH2 were from Merck Millipore. Antibodies for PCNA, total H3, and Ki67 were from Cell Signaling Technology. Antibody for α-SMA was from Sigma Aldrich. Antibodies for p16 ^{INK4A} and GAPDH were from Proteintech. Antibodies for SM22α and α-tubulin were from Santa Cruz Biotechnology. Enhanced chemiluminescence western blotting detection kit was from Thermo Fisher Scientific Corp. Total RNA extraction kit was from Transgene, Beijing, China. Reverse transcription kit was from Thermo Fisher Scientific Corp. SYBR Green PCR master mix was from Transgene, Beijing, China. Magnetic beads for ChIP assay was from Thermo Fisher Scientific Corp.

2.16 | Nomenclature of targets and ligands statement

Key protein targets and ligands in this article are hyperlinked to corresponding entries in http://www.guidetopharmacology.org, the common portal for data from the IUPHAR/BPS Guide to PHARMACOLOGY (Harding et al., 2018), and are permanently archived in the Concise Guide to PHARMACOLOGY 2017/18 (Alexander, Cidlowski, et al., 2017; Alexander, Fabbro, et al., 2017).

3 | RESULTS

3.1 | H3K27me3 level was increased in PDGF-BB-treated VSMCs and injured rat carotid arteries

To study the role of histone methylation during VSMC migration and proliferation, we first used quantitative MS to profile the histone methylation in VSMCs treated with PDGF-BB (40 ng·ml^{-1}, 36 hr). The increase in methylation was the highest for H3K27me3 among all modifications in PDGF-BB-treated cells as compared with untreated control cells (Figure 1a). To further verify this finding, we treated VSMCs with 10% FBS or PDGF-BB and found H3K27me3 level significantly increased as compared with control group (Figure 1b,c). In vivo in rats, at 14 days after carotid artery wire injury for neointimal hyperplasia, H3K27me3 level was increased in the neointima of the carotid artery (Figure 1d). Along with increased H3K27me3 level in injured arteries, the expression of contractile markers of VSMC, including α-SMA and SM-22α, was decreased and that of the proliferative marker PCNA was increased (Figure 1e,f). These results suggest that H3K27me3 may play a role in neointimal formation.

We further tested the change in H3K27me3 level at 0, 3, 7, and 14 days after wire injury in the rat arteries. H3K27me3 level was up-regulated 3 days after wire injury (Figure 2a,b). The methyltransferases EZH2/1, the core component of PRC2, play a crucial role during H3K27 methylation (Margueron & Reinberg, 2011). Although EZH2/1 confers methyltransferase activity during this process, the expression was much lower for EZH1 than for EZH2 in VSMCs (Figure S1A). PRC2 containing EZH1 was reported to have lower methyltransferase activity relative to that containing EZH2 (Margueron & Reinberg, 2011). In addition, we found a similar expression pattern of EZH2 and PCNA as H3K27me3 (Figure 2b,c). Conversely, α-SMA and SM-22α levels were decreased to the lowest at Day 7 post-injury (Figure 2c). Consistent with the in vivo study, EZH2 level was increased after PDGF-BB and FBS treatment in VSMCs (Figure 2d,e). In contrast, PDGF-BB treatment did not affect the protein level of EZH1 (Figure S1B). Thus, carotid artery wire injury and PDGF-BB treatment increased H3K27me3 level by up-regulating the expression of EZH2.

Next, we found that the mRNA level of EZH2 was not changed when treated with PDGF-BB (Figure 2f). Further, when treated with cycloheximide to prevent the translation of proteins, the protein level of EZH2 was declined at 8 hr, which was suppressed by PDGF-BB (Figure 2g). These data indicate that PGDF-BB stabilized EZH2 protein and increased its protein level.

3.2 | Repressed H3K27me3 level suppressed VSMC proliferation

To elucidate the role of increased H3K27me3 level in VSMCs, we treated cells with UNC1999, an inhibitor highly selective for EZH2/1, to inhibit the methyltransferase activity of PRC2. UNC1999 was co-incubated with PDGF-BB for 36 hr after 48-hr serum starvation of VSMCs. UNC1999 concentration-dependently repressed H3K27me3 level induced by PDGF-BB (Figure 3a). The 3-μM UNC1999 reversed the increased in H3K27me3 level induced by PDGF-BB (Figures 3a and S2A), and we used 3-μM UNC1999 for the following in vitro experiments. Then, we characterized the role of UNC1999 in VSMC proliferation. Increased VSMC number induced by PDGF-BB was markedly inhibited by UNC1999 (Figure S2B). Also, the viability of VSMCs was attenuated by UNC1999 treatment (Figure 3b). On immunofluorescence, UNC1999 decreased the number of Ki67-positive cells in PDGF-BB-challenged VSMCs (Figure 3c). Furthermore, flow cytometry revealed fewer cells in the G0-G1 cell phase and more cells in the S phase on PDGF-BB challenge, which was reversed with UNC1999 treatment (Figure 3d,e). Thus, UNC1999 was able to block the S phase entry. Consistently, UNC1999 also blocked the PDGF-BB-induced PCNA expression (Figure 3f,g) and inhibited PDGF-BB-induced VSMC migration (Figure S2C,D).

3.3 | PDGF-BB-induced H3K27me3 suppressed the expression of p16^{INK4A}

The cyclin-dependent kinase inhibitor p16^{INK4A} was reported to be regulated by the polycomb group of chromatin regulators, with EZH2 playing a critical role (Ito, Teo, Evans, Neretti, & Sedivy, 2018).

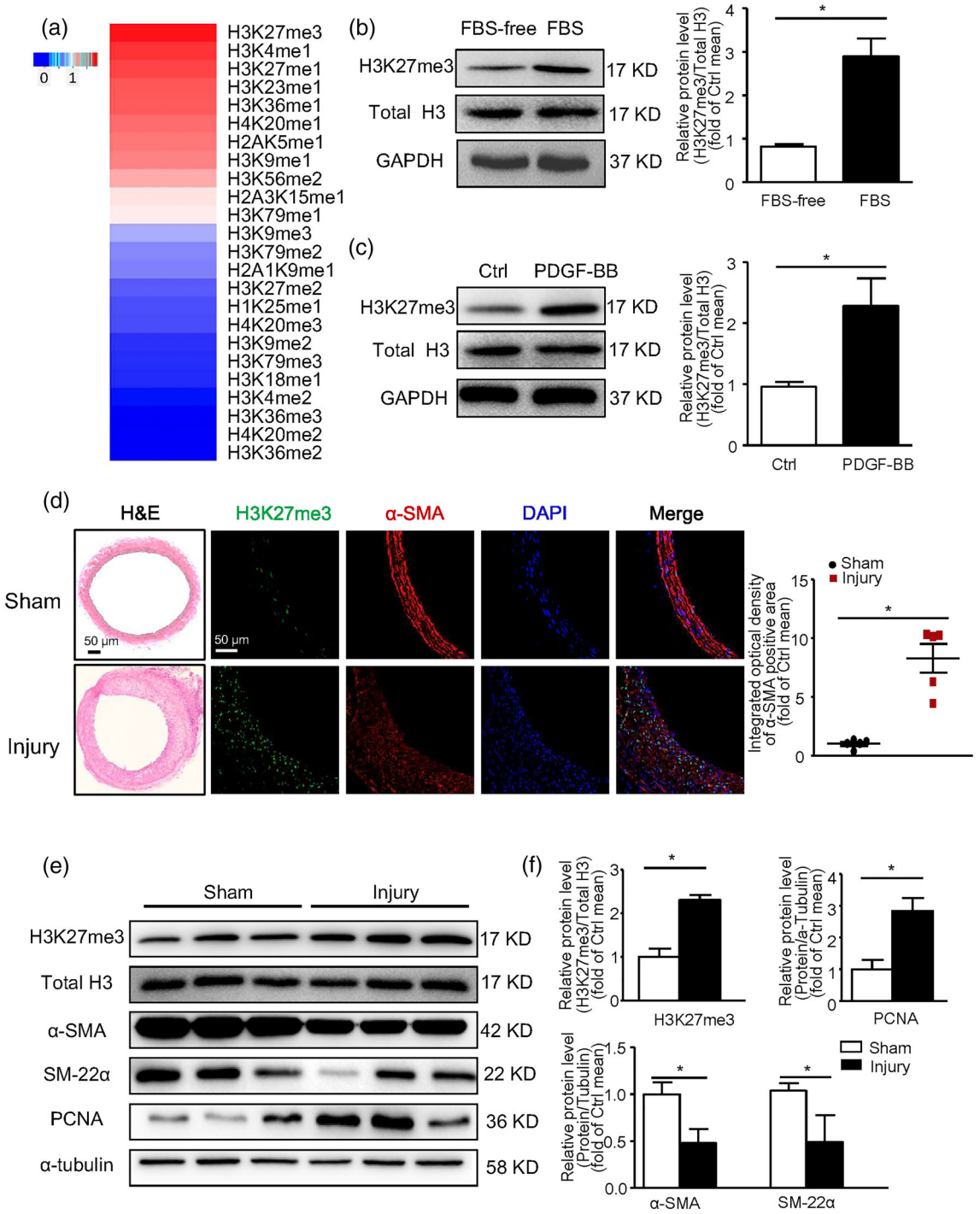

FIGURE 1 Trimethylation of H3K27 was induced in PDGF-BB treated vascular smooth muscle cells (VSMCs) and neointima of rat wire-injured carotid arteries. (a) VSMCs were treated with PDGF-BB (40 ng·ml^{-1}) for 36 hr after serum starvation. Histone methylation was detected by NANO-HPLC/MS. The change in methylation is shown as a heat map. (b,c) VSMCs were treated with 10% FBS (b) or PDGF-BB (40 ng·ml^{-1}) (c) for 36 hr after being starved for 48 hr: western blot analysis of protein levels of H3K27me3, total H3, and GAPDH; data are mean ± SEM, n = 5. (d,e) Rats underwent carotid artery wire injury (n = 5 rats in each group). At 14 days after surgery, arteries were collected. (d) Representative H&E staining and immunostaining of H3K27me3, α-SMA, and DAPI (left panel, scale bar = 50 μm); quantification of mean integrated OD of H3K27me3 in α-SMA positive area (right panel). (e) Western blot analysis of protein levels of H3K27me3, total H3, α-SMA, SM-22, PCNA, and α-tubulin. Data are mean ± SEM. *P < .05. Ctrl, control

P16^{INK4A} arrests VSMC proliferation by preventing G1/S phase progression (Gizard et al., 2008). Thus, we detected enriched H3K27me3 level at the p16^{INK4A} locus by ChIP analysis, indicating that PDGF-BB increased H3K27me3 level within 0.6-kb upstream and 0.5-kb downstream of the promotor of p16^{INK4A} (Figure 4a). Furthermore, p16^{INK4A} mRNA level was significantly suppressed by

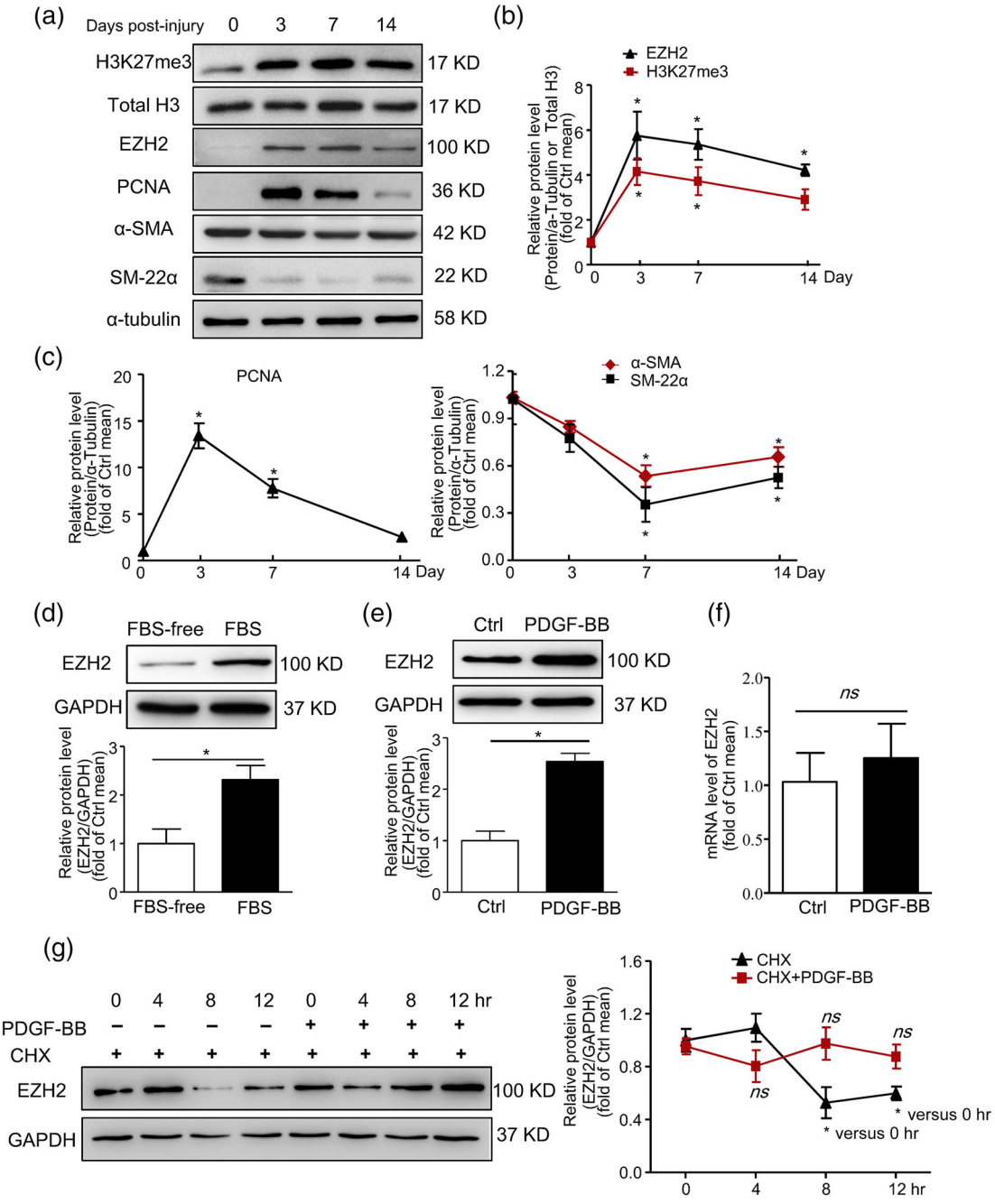

FIGURE 2 Increased expression of EZH2 in injured carotid arteries and PDGF-BB-treated VSMCs. (a–c) Rats underwent carotid wire injury. At Days 0, 3, 7, and 14 post-injury, arteries were collected. (a) Western blot analysis of protein levels of H3K27me3, total H3, EZH2, α-SMA, PCNA, and α-tubulin; (b,c) quantification of (a); n = 5 rats in each group; *P < .05 versus 0 day. (d) VSMCs were treated with 10% FBS for 36 hr after serum starvation: western blot analysis of protein levels of EZH2 and GAPDH; data are mean ± SEM, n = 5. *P < .05. (e,f) VSMCs were treated with PDGF-BB (40 ng·ml^{-1}) for 36 hr after serum starvation: (e) western blot analysis of protein levels of EZH2 and GAPDH; (f) qPCR analysis of the mRNA levels of EZH2; n = 5. *P < .05. (g) VSMCs were treated with cycloheximide (50 ng·ml^{-1}) with or without PDGF-BB (40 ng·ml^{-1}) for 0, 4, 8, and 12 hr, respectively; western blot analysis of protein levels of EZH2 and GAPDH; *P < .05 *versus* 0 hr without PDGF-BB. ns versus 0 hr with PDGF-BB. Data are mean ± SEM. Ctrl, control; CHX, cycloheximide; ns, not significant

PDGF-BB compared with control group, which was reversed by UNC1999 treatment (Figure 4b). In addition, immunofluorescence staining showed a changed protein level of P16^{INK4A} consistent with the mRNA level (Figure 4c). These results indicate that PDGF-BB-induced H3K27me3 promoted VSMC proliferation by repressing p16^{INK4A} expression.

3.4 | Systemic or local administration of UNC1999 protected against carotid artery wire injury-induced neointimal formation

UNC1999 was found orally bioavailable in mice (Konze et al., 2013). Following a single 50 mg·kg^{-1} oral dose of UNC1999, its plasma

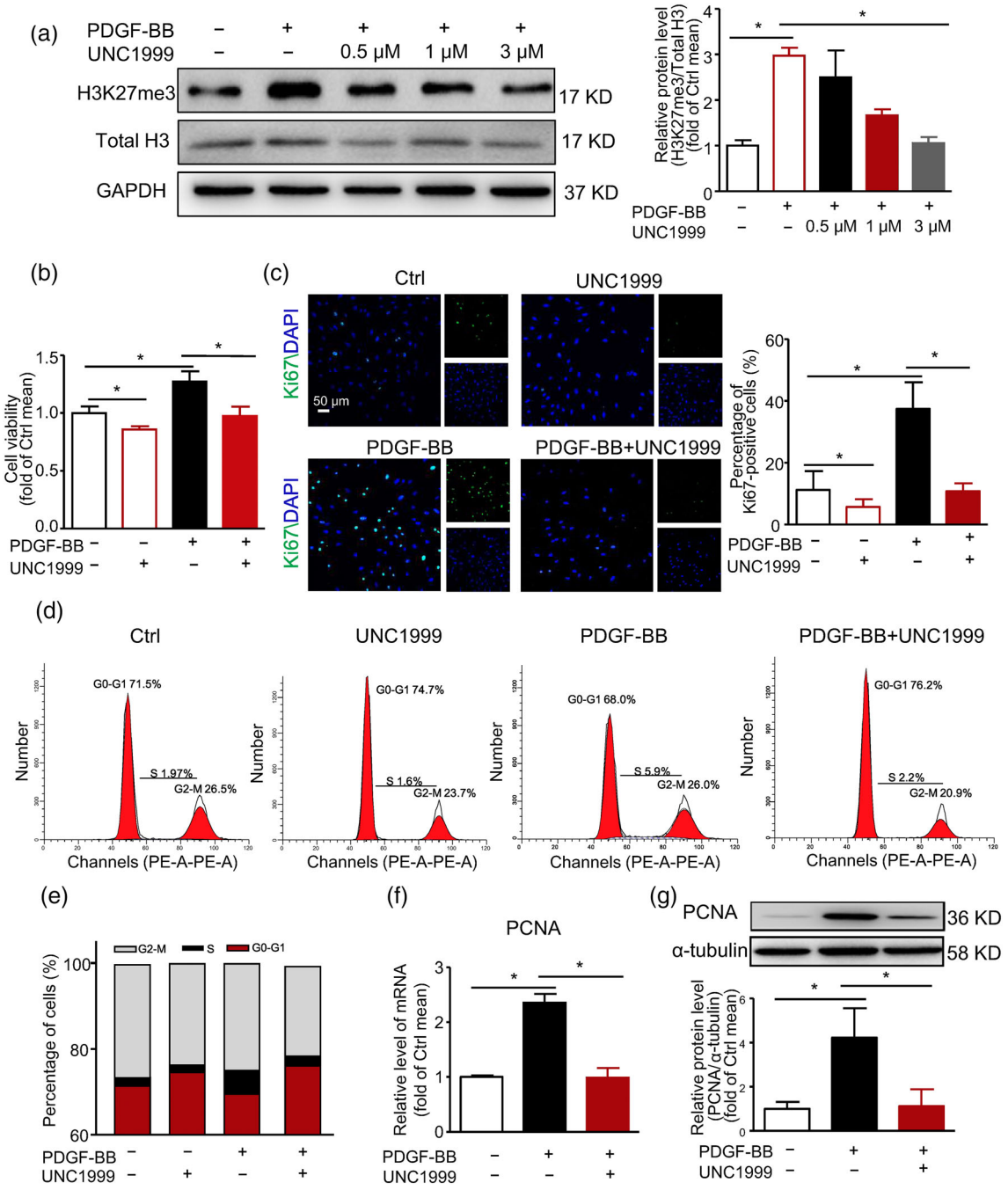

FIGURE 3 UNC1999 prevented PDGF-BB-induced VSMC proliferation. (a) VSMCs were treated with PDGF-BB (40 ng·ml^{-1}) with or without UNC1999 (0.5, 1, and 3 μM, respectively) for 36 hr. Western blot analysis of protein levels of H3K27me3, total H3, and GAPDH. (b–g) VSMCs were treated with PDGF-BB (40 ng·ml^{-1}) with or without UNC1999 (3 μM) for 36 hr. (b) MTS analysis of cell viability. (c) Representative immunofluorescence staining of Ki67 and DAPI (left panel, scale bar = 50 μm); quantification of percentage of Ki67-positive cells (right panel). (d,e) Cell cycle determination by flow cytometry. Levels of mRNA (f) and protein (g) of PCNA. Data are mean ± SEM, n = 5, *P < .05. Ctrl, control

concentration was maintained above its cellular IC_{50} for approximately 20 hr. No adverse effects were observed at this dosage (Konze et al., 2013). Thus, we treated the rats with UNC1999 (50 mg·kg^{-1}·day^{-1}) by gavage for 3 days and found that the BP of these rats were not affected by UNC1999 (Figure S3). Then, we treated rats with 50 mg·kg^{-1}·day^{-1} UNC1999 at 1 day before carotid artery wire injury and lasting for 15 days (Figure 5a). As compared with the injured arteries, UNC1999 significantly suppressed carotid artery wire injury-up-regulated H3K27me3 (Figure 5b). At Day 14 post-injury, neointimal formation was attenuated by UNC1999, as evidenced by H&E staining (Figure 5c) and EVG staining (Figure S4A). UNC1999 markedly reduced the neointimal area and ratio of neointima to media area of injured arteries. However, media area and circumference of external elastic lamina were comparable between the groups (Figures 5c and S4A).

To further explore the therapeutic potential of UNC1999 as a stent-coating drug, we studied the local effects of UNC1999 on

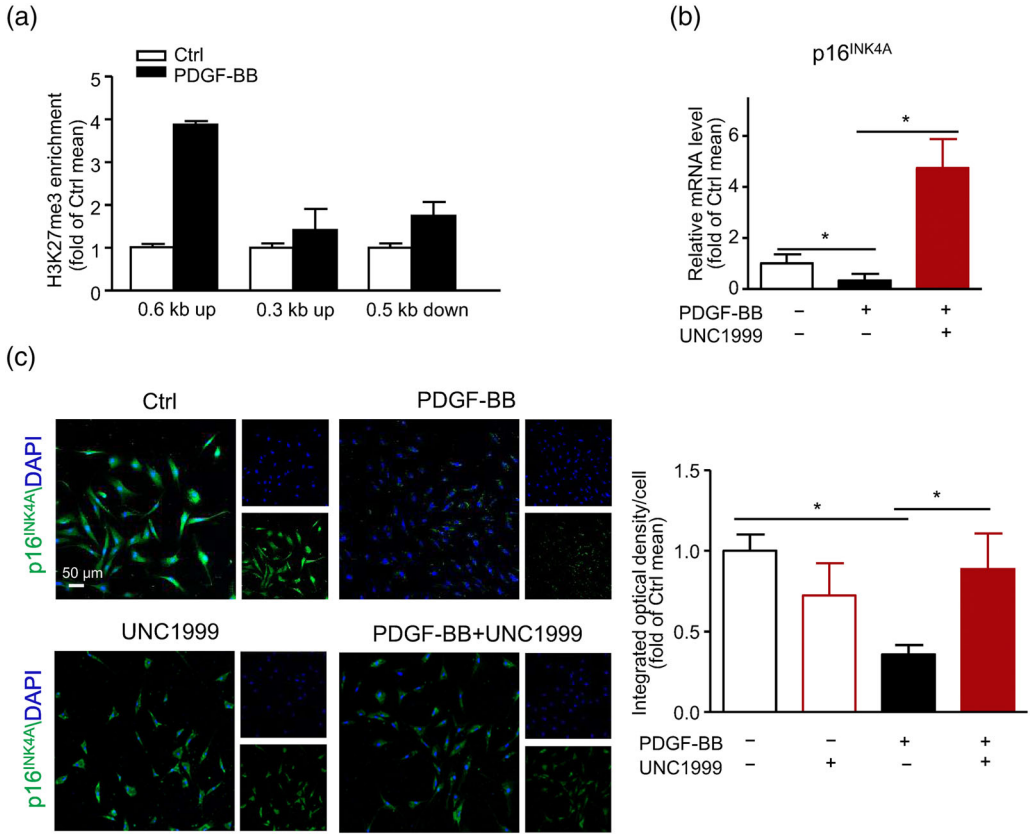

FIGURE 4 PDGF-BB-induced increase in H3K27me3 suppressed the expression of $p16^{INK4A}$. VSMCs were treated with PDGF-BB (40 ng·ml^{-1}) with or without UNC1999 (3 μM) for 36 hr. (a) ChIP analysis of the increase in H3K27me3 at the locus; data are mean ± SEM, n = 3. (b) qPCR analysis of the mRNA level of $p16^{INK4A}$. (c) Representative immunofluorescence staining of $p16^{INK4A}$ (left panel, scale bar = 50 μm) and quantification of mean integrated OD of $p16^{INK4A}$ per cell (right panel). (b,c) Data are mean ± SEM, n = 5, *P < .05. Ctrl, control

injured arteries. We applied 50 mg·kg^{-1} body weight UNC1999 mixed with 30% PF127 gel perivascularly by mixing it in pluronic gel immediately after wire injury surgery (Figure 5d). Similar to oral administration of UNC1999, perivascular delivery significantly ameliorated injury-induced neointimal formation in comparison with injured arteries, as evidenced by reduced neointima area and ratio of neointima to media area (Figures 5e,f and S4B). Again, media area and circumference of external elastic lamina were not affected by the surgery and UNC1999 application (Figures 5f and S4B). Consistent with the in vitro study, $p16^{INK4A}$ level was decreased markedly 14 days after wire injury and recovered by systemic or local application of UNC1999 (Figure 6a,b). Thus, our results suggest that UNC1999 could prevent carotid artery wire injury-induced neointimal formation systemically and locally.

4 | DISCUSSION

Restenosis, a serious complication occurring after angioplasty or in-stent surgery for arterial narrowing diseases, is involved in various life-threatening conditions, such as heart infarction and stroke (Boulanger et al., 2015). Here, we found that levels of H3K27me3, a gene expression silencer, and its specific regulator EZH2 were increased in VSMCs implicated in neointimal formation. With oral or perivascular administration of UNC1999, an inhibitor of EZH2/1, neointimal formation was markedly attenuated in vivo in rats. In vitro, UNC1999 was able to inhibit VSMC proliferation. Mechanistically, elevated EZH2 level up-regulated H3K27me3, which in turn inhibited the transcription of $p16^{INK4A}$ and promoted VSMC proliferation (Figure 7).

Enrichment of H3K27me3 on chromatin leads to gene silencing, which is more important for maintaining gene repression than H3K27 dimethylation in vivo (Margueron & Reinberg, 2011). H3K27 methylation is specifically catalysed by PRC2 containing the EZH2 catalytic subunit, which has higher methyltransferase activity than that containing EZH1 (Margueron & Reinberg, 2011). Our data revealed higher expression of EZH2 than EZH1 in VSMCs, which suggests that EZH2 is the dominant catalytic subunit in VSMCs. Furthermore, protein level of EZH2 was increased and that of EZH1 was not changed in VSMCs by PDGF-BB treatment. Thus, the increased H3K27me3 level in PDGF-BB-treated VSMCs was mainly mediated by EZH2. EZH2-mediated trimethylation of H3K27 plays important roles in cancer and cardiovascular diseases. Inhibition of EZH2 improved thoracic aortic aneurysm in a mouse model of Marfan syndrome (Lino Cardenas et al., 2018). EZH2 mediated the inflammatory responses of VSMCs to tumour necrosis factor α stimulation (Shu et al., 2017). Also,

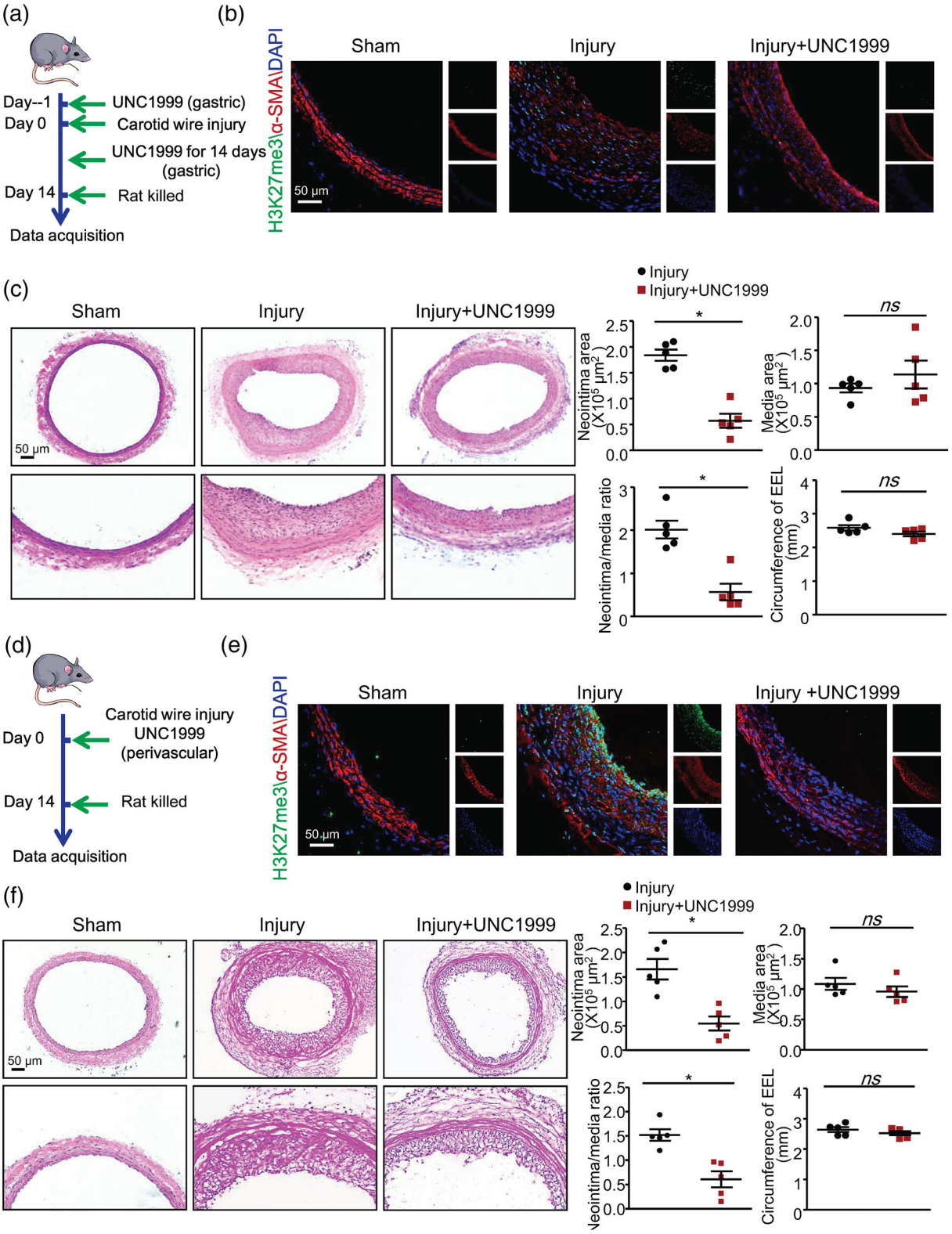

FIGURE 5 Systemic or local application of UNC1999 attenuated neointimal formation induced by wire injury. (a–c) Rats underwent oral gavage with 50 mg·kg^{-1}·day^{-1} UNC1999 at 1 day before wire injury and continued for 15 days. (d–f) Rats underwent perivascular application of UNC1999 (50 mg·kg^{-1}) immediately after the wire injury and were killed 14 days after the wire injury. (a,d) Schematic representation of the treatment. (b,e) Representative immunofluorescence staining of H3K27me3, α-SMA, and DAPI (scale bar = 50 μm). (c,f) H&E staining showing the neointimal formation and quantification of neointima, media area, ratio of neointima to media area, and circumference of external elastic lamina; scale bar = 50 μm. Data are mean ± SEM, n = 5 rats in each group, *P < .05. ns, not significant

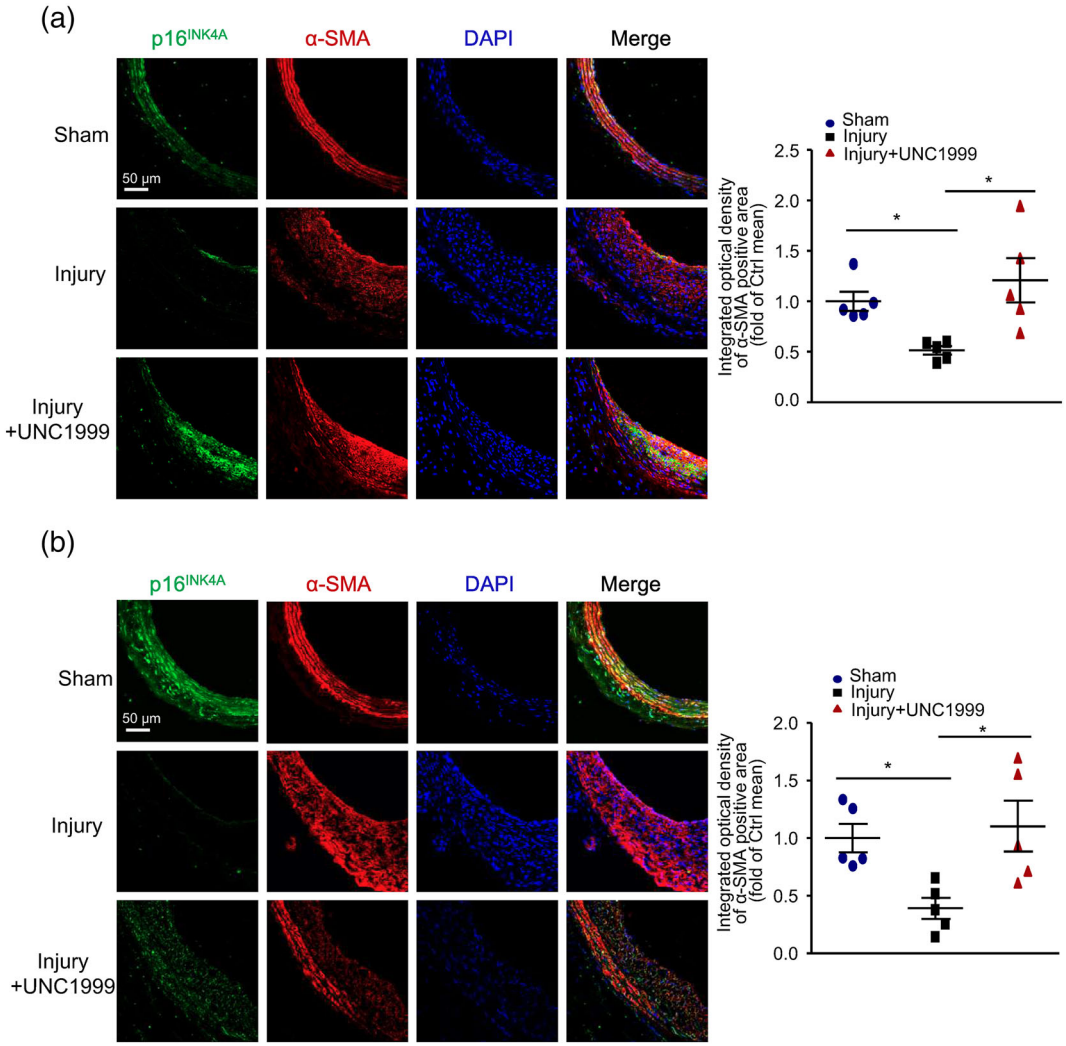

FIGURE 6 $p16^{INK4A}$ expression in VSMCs was decreased after wire injury and reversed by UNC1999 treatment. (a) Rats underwent oral gavage with 50 $mg \cdot kg^{-1} \cdot day^{-1}$ UNC1999 at 1 day before wire injury and lasting for 15 days. (b) Rats underwent perivascular application of UNC1999 (50 $mg \cdot kg^{-1}$) immediately after the wire injury and were killed at 14 days after wire injury. Representative immunofluorescence staining of $p16^{INK4A}$, α-SMA, and DAPI (left panel, scale bar = 50 μm) and quantification of mean integrated OD of $p16^{INK4A}$ in α-SMA-positive area (right panel). n = 5 rats in each group; data are mean ± SEM, $^*P < .05$

hyperhomocysteinaemia, a risk factor of atherosclerosis, up-regulated the expression of EZH2 in the aorta of $ApoE^{-/-}$ mice (Xiaoling et al., 2016). In VSMCs, decreased EZH2 expression induced excessive autophagosome formation and thus accelerated aortic dissection occurrence (Li, Yi, et al., 2018). In our study, we found that EZH2 level increased in VSMCs implicated in injured carotid arteries and cultured VSMCs treated with PDGF-BB. Inhibiting the catalytic activity of EZH2 with a specific inhibitor ameliorated the neointimal formation by attenuating VSMC proliferation.

$p16^{INK4A}$, a critical cyclin-dependent kinase inhibitor, has inhibitory effects on VSMC proliferation. Gizard et al. (2005) and Gizard et al. (2008) reported that **PPAR-α** protected against intimal hyperplasia by inducing $p16^{INK4A}$ expression (Gizard et al., 2005; Gizard et al., 2008). Also, dehydroepiandrosterone sulfate up-regulated $p16^{INK4A}$ and thereby inhibited VSMC proliferation (Ii et al., 2009). In contrast, 9p21.3 risk variants for coronary artery disease in human aortic SMCs were found associated with reduced $p16^{INK4A}$ level and increased SMC proliferation (Almontashiri et al., 2015). Of note, $p16^{INK4A}$ was reported to be regulated by EZH2. Loss of EZH2 induced $p16^{INK4A}$ by reducing H3K27me3 enrichment (Chen et al., 2018; Ito et al., 2018). Thus, we detected $p16^{INK4A}$ in VSMCs under different treatments. PDGF-BB reduced its expression, which was reversed by UNC1999. Consistent with in vitro study, carotid artery injury in rats decreased $p16^{INK4A}$ in VSMCs, which was reversed by UNC1999 application. These data suggest that increased H3K27me3 level promoted VSMC proliferation by reducing $p16^{INK4A}$ expression.

We demonstrated that UNC1999 largely ameliorated restenosis by oral application and also perivascular delivery. Despite no adverse effects observed in mice when UNC1999 was orally delivered, EZH2/1 has multiple effects on various tissues other than arteries. Thus, we found that UNC1999 could be delivered and sustained locally to prevent restenosis. The effects of UNC1999 when it was applied via perivascular delivery to injured arteries demonstrated that it has potential as a stent-coating drug for restenosis. However, the

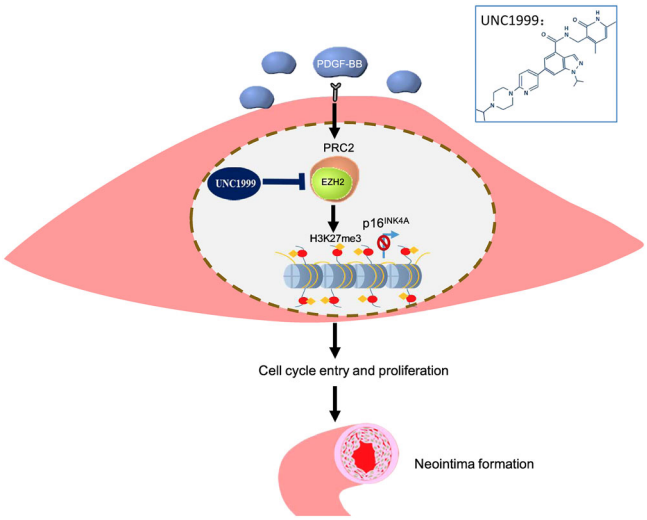

FIGURE 7 Proposed mechanism through which H3K27m3 promotes restenosis. PDGF-BB increases H3K27me3 level by up-regulating EZH2. The increase in H3K27me3 inhibits the transcription of $p16^{INK4A}$ and promotes VSMC proliferation and neointimal formation

local concentration of UNC1999 was not determined because of technical limitations, which is a limitation of the presented study.

In summary, we showed that the level of H3K27me3 was increased during neointimal formation after wire injury to rat carotid arteries, which was associated with increased expression of EZH2. Mechanistically, this increased H3K27me3 level inhibited the transcription of $p16^{INK4A}$ and de-repressed VSMC proliferation. Inhibiting PRC2 activity by UNC1999 systemically or locally protected against restenosis. Our results indicate that PRC2 inhibitors have potential as candidate drugs for restenosis.

ACKNOWLEDGEMENT

This work was supported by the National Natural Science Foundation of China (81730014, 81822006, 81770836, 81790621, and 91539108).

CONFLICT OF INTEREST

The authors declare no conflicts of interest.

AUTHOR CONTRIBUTIONS

J.L. contributed to the concept and design, data acquisition, analysis and interpretation, and drafting of the article. Q.L. contributed to the data acquisition, analysis and interpretation, and drafting of the article. W.C., X.Z., B.Y., X.L., S.J., S.T., K.Z., and H.S. contributed to the data acquisition of the article. D.A. contributed to the concept and design of the article. X.Z., C.W., and Y.Z. contributed to the concept and design, data acquisition, analysis and interpretation, and drafting of the article. X.Z., C.W., and Y.Z. are the guarantors of the work.

DECLARATION OF TRANSPARENCY AND SCIENTIFIC RIGOUR

This Declaration acknowledges that this paper adheres to the principles for Transparency and Scientific Rigour as stated in the BJP guidelines for Design and Analysis, Immunoblotting and immunohistochemistry, and Design and Analysis, and as recommended by funding agencies, publishers and other organisations engaged with supporting research.

ORCID

Yi Zhu https://orcid.org/0000-0001-7725-9166

REFERENCES

Ai, S., Yu, X., Li, Y., Peng, Y., Li, C., Yue, Y., … He, A. (2017). Divergent requirements for EZH1 in heart development versus regeneration. *Circulation Research*, *121*(2), 106–112. https://doi.org/10.1161/CIRCRESAHA.117.311212

Alexander, S. P., Cidlowski, J. A., Kelly, E., Marrion, N. V., Peters, J. A., Faccenda, E., … CGTP Collaborators. (2017). The Concise Guide to PHARMACOLOGY 2017/18: Nuclear hormone receptors. *British Journal of Pharmacology*, *174*(Suppl 1), S208–S224. https://doi.org/10.1111/bph.13880

Alexander, S. P., Fabbro, D., Kelly, E., Marrion, N. V., Peters, J. A., Faccenda, E., … CGTP Collaborators. (2017). The Concise Guide to PHARMACOLOGY 2017/18: Enzymes. *British Journal of Pharmacology*, *174*(Suppl 1), S272–S359.

Aljubran, S. A., Cox, R. Jr., Tamarapu Parthasarathy, P., Kollongod Ramanathan, G., Rajanbabu, V., Bao, H., … Kolliputi, N. (2012). Enhancer of zeste homolog 2 induces pulmonary artery smooth muscle cell proliferation. *PLoS ONE*, *7*(5), e37712. https://doi.org/10.1371/journal.pone.0037712

Almontashiri, N. A., Antoine, D., Zhou, X., Vilmundarson, R. O., Zhang, S. X., Hao, K. N., … Stewart, A. F. (2015). 9p21.3 coronary artery disease risk variants disrupt TEAD transcription factor-dependent transforming growth factor β regulation of p16 expression in human aortic smooth muscle cells. *Circulation*, *132*(21), 1969–1978.

Boulanger, M., Cameliere, L., Felgueiras, R., Berger, L., Rerkasem, K., Rothwell, P. M., & Touzé, E. (2015). Periprocedural myocardial infarction after carotid endarterectomy and stenting: Systematic review and meta-analysis. *Stroke*, *46*(10), 2843–2848. https://doi.org/10.1161/STROKEAHA.115.010052

Cai, Y., Nagel, D. J., Zhou, Q., Cygnar, K. D., Zhao, H., Li, F., … Yan, C. (2015). Role of cAMP-phosphodiesterase 1C signaling in regulating growth factor receptor stability, vascular smooth muscle cell growth, migration, and neointimal hyperplasia. *Circulation Research*, *116*(7), 1120–1132. https://doi.org/10.1161/CIRCRESAHA.116.304408

Cao, Y., Lu, L., Liu, M., Li, X. C., Sun, R. R., Zheng, Y., & Zhang, P. Y. (2014). Impact of epigenetics in the management of cardiovascular disease: A review. *European Review for Medical and Pharmacological Sciences*, *18*(20), 3097–3104.

Chen, G., Subedi, K., Chakraborty, S., Sharov, A., Lu, J., Kim, J., … Weng, N. P. (2018). Ezh2 regulates activation-induced CD8(+) T cell cycle progression via repressing Cdkn2a and Cdkn1c expression. *Frontiers in Immunology*, *9*, 549. https://doi.org/10.3389/fimmu.2018.00549

Conway, E., Healy, E., & Bracken, A. P. (2015). PRC2 mediated H3K27 methylations in cellular identity and cancer. *Current Opinion in Cell Biology*, *37*, 42–48. https://doi.org/10.1016/j.ceb.2015.10.003

Curtis, M. J., Alexander, S., Cirino, G., Docherty, J. R., George, C. H., Giembycz, M. A., … Ahluwalia, A. (2018). Experimental design and analysis and their reporting II: Updated and simplified guidance for authors and peer reviewers. *British Journal of Pharmacology*, *175*(7), 987–993. https://doi.org/10.1111/bph.14153

Dambacher, S., Hahn, M., & Schotta, G. (2010). Epigenetic regulation of development by histone lysine methylation. *Heredity (Edinb)*, *105*(1), 24–37. https://doi.org/10.1038/hdy.2010.49

Gizard, F., Amant, C., Barbier, O., Bellosta, S., Robillard, R., Percevault, F., … Staels, B. (2005). PPAR α inhibits vascular smooth muscle cell proliferation underlying intimal hyperplasia by inducing the tumor suppressor p16INK4a. *The Journal of Clinical Investigation*, *115*(11), 3228–3238. https://doi.org/10.1172/JCI22756

Gizard, F., Nomiyama, T., Zhao, Y., Findeisen, H. M., Heywood, E. B., Jones, K. L., … Bruemmer, D. (2008). The PPARα/p16INK4a pathway inhibits vascular smooth muscle cell proliferation by repressing cell cycle-dependent telomerase activation. *Circulation Research*, *103*(10), 1155–1163. https://doi.org/10.1161/CIRCRESAHA.108.186205

Harding, S. D., Sharman, J. L., Faccenda, E., Southan, C., Pawson, A. J., Ireland, S., Davies, J. A., … NC-IUPHAR. (2018). The IUPHAR/BPS guide to pharmacology in. *Updates and expansion to encompass the new guide to immunopharmacology*. *Nucl Acids Res*, *46*, D1091–D1106. https://doi.org/10.1093/nar/gkx1121

He, J., Bao, Q., Yan, M., Liang, J., Zhu, Y., Wang, C., & Ai, D. (2018). The role of Hippo/yes-associated protein signalling in vascular remodelling associated with cardiovascular disease. *British Journal of Pharmacology*, *175*(8), 1354–1361. https://doi.org/10.1111/bph.13806

Herrington, W., Lacey, B., Sherliker, P., Armitage, J., & Lewington, S. (2016). Epidemiology of atherosclerosis and the potential to reduce the global burden of atherothrombotic disease. *Circulation Research*, *118*(4), 535–546. https://doi.org/10.1161/CIRCRESAHA.115.307611

Igata, M., Motoshima, H., Tsuruzoe, K., Kojima, K., Matsumura, T., Kondo, T., … Araki, E. (2005). Adenosine monophosphate-activated protein kinase suppresses vascular smooth muscle cell proliferation through the inhibition of cell cycle progression. *Circulation Research*, *97*(8), 837–844. https://doi.org/10.1161/01.RES.0000185823.73556.06

Ii, M., Hoshiga, M., Negoro, N., Fukui, R., Nakakoji, T., Kohbayashi, E., … Ohsawa, N. (2009). Adrenal androgen dehydroepiandrosterone sulfate inhibits vascular remodeling following arterial injury. *Atherosclerosis*, *206*(1), 77–85. https://doi.org/10.1016/j.atherosclerosis.2009.02.021

Ito, T., Teo, Y. V., Evans, S. A., Neretti, N., & Sedivy, J. M. (2018). Regulation of cellular senescence by polycomb chromatin modifiers through distinct DNA damage- and histone methylation-dependent pathways. *Cell Reports*, *22*(13), 3480–3492. https://doi.org/10.1016/j.celrep.2018.03.002

Jain, M., Singh, A., Singh, V., & Barthwal, M. K. (2015). Involvement of interleukin-1 receptor-associated kinase-1 in vascular smooth muscle cell proliferation and neointimal formation after rat carotid injury. *Arteriosclerosis, Thrombosis, and Vascular Biology*, *35*(6), 1445–1455. https://doi.org/10.1161/ATVBAHA.114.305028

Kilkenny, C., Browne, W., Cuthill, I. C., Emerson, M., & Altman, D. G. (2010). Animal research: Reporting in vivo experiments: the ARRIVE guidelines. *British Journal of Pharmacology*, *160*, 1577–1579.

Konze, K. D., Ma, A., Li, F., Barsyte-Lovejoy, D., Parton, T., Macnevin, C. J., … Jin, J. (2013). An orally bioavailable chemical probe of the lysine methyltransferases EZH2 and EZH1. *ACS Chemical Biology*, *8*(6), 1324–1334. https://doi.org/10.1021/cb400133j

Leentjens, J., Bekkering, S., Joosten, L. A. B., Netea, M. G., Burgner, D. P., & Riksen, N. P. (2018). Trained innate immunity as a novel mechanism linking infection and the development of atherosclerosis. *Circulation Research*, *122*(5), 664–669. https://doi.org/10.1161/CIRCRESAHA.117.312465

Li, L., Liu, X., He, L., Yang, J., Pei, F., Li, W., … Sun, L. (2017). ZNF516 suppresses EGFR by targeting the CtBP/LSD1/CoREST complex to chromatin. *Nature Communications*, *8*(1), 691. https://doi.org/10.1038/s41467-017-00702-5

Li, Q., Liao, C., Xu, W., Li, G., Hong, K., Cheng, X., & Li, J. (2018). Xeroderma pigmentosum group D (XPD) inhibits the proliferation cycle of vascular smooth muscle cell (VSMC) by activating glycogen synthase kinase 3β (GSK3β). *Medical Science Monitor: International Medical Journal of Experimental and Clinical Research*, *24*, 5951–5959. https://doi.org/10.12659/MSM.909614

Li, R., Yi, X., Wei, X., Huo, B., Guo, X., Cheng, C., … Jiang, D. S. (2018). EZH2 inhibits autophagic cell death of aortic vascular smooth muscle cells to affect aortic dissection. *Cell Death & Disease*, *9*(2), 180. https://doi.org/10.1038/s41419-017-0213-2

Lino Cardenas, C. L., Kessinger, C. W., MacDonald, C., Jassar, A. S., Isselbacher, E. M., Jaffer, F. A., & Lindsay, M. E. (2018). Inhibition of the methyltranferase EZH2 improves aortic performance in experimental thoracic aortic aneurysm. *JCI Insight*, *3*(5). https://doi.org/10.1172/jci.insight.97493

Liu, D., Huang, Y., Bu, D., Liu, A. D., Holmberg, L., Jia, Y., … Jin, H. (2014). Sulfur dioxide inhibits vascular smooth muscle cell proliferation via suppressing the Erk/MAP kinase pathway mediated by cAMP/PKA signaling. *Cell Death & Disease*, *5*, e1251. https://doi.org/10.1038/cddis.2014.229

Liu, R., Bauer, A. J., & Martin, K. A. (2016). A new editor of smooth muscle phenotype. *Circulation Research*, *119*(3), 401–403. https://doi.org/10.1161/CIRCRESAHA.116.309218

Margueron, R., & Reinberg, D. (2011). The polycomb complex PRC2 and its mark in life. *Nature*, *469*(7330), 343–349. https://doi.org/10.1038/nature09784

Maruo, S., Zhao, B., Johannsen, E., Kieff, E., Zou, J., & Takada, K. (2011). Epstein-Barr virus nuclear antigens 3C and 3A maintain lymphoblastoid cell growth by repressing p16INK4A and p14ARF expression. *Proceedings of the National Academy of Sciences of the United States of America*, *108*(5), 1919–1924. https://doi.org/10.1073/pnas.1019599108

Moritz, L. E., & Trievel, R. C. (2018). Structure, mechanism, and regulation of polycomb-repressive complex 2. *The Journal of Biological Chemistry*, *293*(36), 13805–13814. https://doi.org/10.1074/jbc.R117.800367

Shu, Y. N., Dong, L. H., Li, H., Pei, Q. Q., Miao, S. B., Zhang, F., … Han, M. (2017). CKII-SIRT1-SM22α loop evokes a self-limited inflammatory response in vascular smooth muscle cells. *Cardiovascular Research*, *113*(10), 1198–1207. https://doi.org/10.1093/cvr/cvx048

Song, T. F., Huang, L. W., Yuan, Y., Wang, H. Q., He, H. P., Ma, W. J., … Zhang, T. C. (2018). LncRNA MALAT1 regulates smooth muscle cell phenotype switch via activation of autophagy. *Oncotarget*, *9*(4), 4411–4426. https://doi.org/10.18632/oncotarget.23230

Wang, L., Zheng, J., Bai, X., Liu, B., Liu, C. J., Xu, Q., … Wang, X. (2009). ADAMTS-7 mediates vascular smooth muscle cell migration and neointimal formation in balloon-injured rat arteries. *Circulation Research*, *104*(5), 688–698. https://doi.org/10.1161/CIRCRESAHA.108.188425

Wang, Q., Huo, L., He, J., Ding, W., Su, H., Tian, D., … Zhu, Y. (2015). Soluble epoxide hydrolase is involved in the development of atherosclerosis and arterial neointimal formation by regulating smooth muscle cell migration. *American Journal of Physiology. Heart and Circulatory Physiology*, *309*(11), H1894–H1903. https://doi.org/10.1152/ajpheart.00289.2015

Wang, Y., Chen, D., Zhang, Y., Wang, P., Zheng, C., Zhang, S., … Kong, W. (2018). Novel adipokine, FAM19A5, inhibits neointimal formation after injury through sphingosine-1-phosphate receptor 2. *Circulation*, *138*(1), 48–63.

Xiaoling, Y., Li, Z., ShuQiang, L., Shengchao, M., Anning, Y., Ning, D., … Yideng, J. (2016). Hyperhomocysteinemia in ApoE$^{-/-}$ mice leads to

overexpression of enhancer of zeste homolog 2 via miR-92a regulation. *PLoS ONE*, *11*(12), e0167744. https://doi.org/10.1371/journal.pone.0167744

Yao, L., Wang, C., Zhang, X., Peng, L., Liu, W., Zhang, X., … Zhu, Y. (2016). Hyperhomocysteinemia activates the aryl hydrocarbon receptor/CD36 pathway to promote hepatic steatosis in mice. *Hepatology*, *64*(1), 92–105. https://doi.org/10.1002/hep.28518

Yuan, Z. F., Lin, S., Molden, R. C., Cao, X. J., Bhanu, N. V., Wang, X., … Garcia, B. A. (2015). EpiProfile quantifies histone peptides with modifications by extracting retention time and intensity in high-resolution mass spectra. *Molecular & Cellular Proteomics: MCP*, *14*(6), 1696–1707. https://doi.org/10.1074/mcp.M114.046011

Zhang, K., Li, L., Zhu, M., Wang, G., Xie, J., Zhao, Y., … Li, E. (2015). Comparative analysis of histone H3 and H4 post-translational modifications of esophageal squamous cell carcinoma with different invasive capabilities. *Journal of Proteomics*, *112*, 180–189. https://doi.org/10.1016/j.jprot.2014.09.004

SUPPORTING INFORMATION

Additional supporting information may be found online in the Supporting Information section at the end of the article.

How to cite this article: Liang J, Li Q, Cai W, et al. Inhibition of polycomb repressor complex 2 ameliorates neointimal hyperplasia by suppressing trimethylation of H3K27 in vascular smooth muscle cells. *Br J Pharmacol*. 2019;176:3206–3219. https://doi.org/10.1111/bph.14754